Magneto-infrared modes in InAs-AlSb-GaSb coupled quantum wells

L.-C. Tung,[1] P. A. Folkes,[2] Godfrey Gumbs,[3] W. Xu,[4,5] and Y.-J. Wang[1]

[1]*National High Magnetic Laboratory, Tallahassee, Florida 32310, USA*
[2]*U.S. Army Research Laboratory, Adelphi, Maryland 20783, USA*
[3]*Hunter College, City University of New York, New York, New York 10021, USA*
[4]*Institute of Solid State Physics, Chinese Academy of Sciences, Hefei 23031, China*
[5]*Yunnan University, Kunming 650091, China*

We have studied a series of InAs/GaSb coupled quantum wells using magneto-infrared spectroscopy for high magnetic fields up to 33 T within temperatures ranging from 4 to 45 K in both Faraday and tilted field geometries. This type of coupled quantum wells consists of an electron layer in the InAs quantum well and a hole layer in the GaSb quantum well, forming the so-called two-dimensional electron-hole bilayer system. Unlike the samples studied in the past, the hybridization of the electron and hole subbands in our samples is largely reduced by having narrower wells and an AlSb barrier layer interposed between the InAs and the GaSb quantum wells, rendering them weakly hybridized. Previous studies have revealed multiple absorption modes near the electron cyclotron resonance of the InAs layer in moderately and strongly hybridized samples while only a single absorption mode was observed in the weakly hybridized samples. We have observed a pair of absorption modes occurring only at magnetic fields higher than 14 T, which exhibited several interesting phenomena. Among which we found two unique types of behavior that distinguish this work from the ones reported in the literature. This pair of modes is very robust against rising thermal excitations and increasing magnetic fields aligned parallel to the heterostructures. While the previous results were aptly explained by the antilevel crossing due to the hybridization of the electron and hole wave functions, i.e., conduction-valence Landau-level mixing, the unique features reported in this paper cannot be explained within the same concept. The unusual properties found in this study and their connection to the known models for InAs/GaSb heterostructures will be discussed; in addition, several alternative ideas will be proposed in this paper and it appears that a spontaneous phase separation can account for most of the observed features.

I. INTRODUCTION

Bose-Einstein condensate (BEC) is a highly ordered state in which the wave-function phase is coherent over distances much longer than the separation between individual particles. BEC of excitons in semiconductors has been a subject of intense interest for decades. In semiconductors, an electron in the conduction band and a hole in the valence band can bind together by Coulomb interaction to form an exciton, a composite boson in contrast to electrons in superconductors, which bind together to form Cooper pairs.[1] While BEC and superconductivity were found in superconductors, excitons in semiconductors have the potential to reach BEC, collective ground states or even superfluidity. This concept has been discussed for three-dimensional (3D) bulk materials,[2–13] and also for two-dimensional (2D) bilayer heterostructures.[14–35] Several phenomena or collective states have been proposed, including exciton insulator,[3–6,8,9,21] gas-liquid-type phase transition,[7] BEC of magnetoexcitons,[2,16,20,22,28,29,31,33,34] electric dipole density wave,[15] electron-hole magnetoplasma,[23] double charge-density-wave state,[24] and most interestingly superfluidity.[10,12,32,35]

Signatures possibly resulting from the BE statistics of excitons have been observed in several bulk systems, such as Ge, CuCl, CuO_2 and in a form of ferromagnetism in $La_xCa_{1-x}B_6$ and $La_xSr_xB_6$.[36–40] Excitons are usually created by shining light on the semiconductor, which creates excess electrons and holes in equal numbers. Optically generated excitons are ephemeral and decay quickly via emission of light. Rapid recombination of electrons and holes tends to destroy the coherence of the excitonic states.[25] The lifetime of the excitons in 3D semiconductors is usually shorter than the thermalization and condensate time, making it difficult to investigate BEC or BE statistics in 3D systems. On the other hand, the lifetime of excitons in 2D heterostructures can be enhanced if the rate of recombination is reduced by spatially separating electrons and holes.[41] Electrons and holes can be confined in different layers between which tunneling can be made negligible by inserting a barrier.[42,43] Though this process reduces Coulomb interaction, and thus a lower critical temperature T_C, confinement of both electrons and holes increases exciton binding energy compared to its value in 3D bulk systems.[25]

It is by far, most favorable to form an electron-hole droplet in a homogeneous bulk semiconductor, which is an insulator;[3–6,9] however, superconductivity or superfluidity are, in principle, possible in bilayer heterostructures.[14,20,27,32] The spatial separation causes the excitons to act like oriented electric dipoles, which have repulsive interactions between each other, preventing the electrons and holes from agglomerating into a universal electron-hole plasma.[33] It has been suggested that the interaction leading to the formation of the droplet can be suppressed by a strong magnetic field[10,12] or sophisticated heterostructures.[28,35] However, one should note that it is generally believed that an ideal BEC is not allowed in a true 2D system, so other interesting phenomena such as

Berezinskii-Kosterlitz-Thouless transition can also be expected.[44,45]

With the advantages over a 3D bulk system and via the modern crystal growth techniques[41,42] such as molecular-beam epitaxy, coupled quantum-well (CQW) heterostructures have emerged as a promising candidate for achieving exciton BEC in semiconductors.[41,46–53] The CQW consists of two low-band-gap well layers separated by a high-band-gap barrier layer. Photoexcited indirect excitons are formed between the holes in the valence band of one layer and the electrons in the conduction band of the other. These excitons carry electric dipoles which are aligned perpendicular to the QW plane, stabilizing excitonic states against the formation of droplets,[22,28] reinforcing the BEC (Ref. [54]) and resulting in the screening of an in-plane potential.[48] Recent discoveries in CQW heterostructures have revealed several interesting phenomena leading to an exciton BEC state in semiconductors.[41,46–53] Others have found exciton-polariton BEC by using a microcavity to couple heavy-hole excitons to cavity photons.[55–61] A list of several BEC systems and their properties was reviewed by Keeling and Berloff recently.[62]

Among the candidates possibly reaching exciton BEC in 2D systems, InAs/GaSb CQW has a unique type-II band alignment, in which the bottom of the conduction band in bulk InAs lies below the top of the valence band in bulk GaSb (i.e., negative effective band gap $E_g \sim -150$ to -180 meV).[63,64] The overlap of electron and hole band edges can spontaneously form excitons without photoexcitations if the single-particle energy gap is smaller than the exciton binding energy. These spontaneously formed excitons have no recombination, and hence, possess long lifetimes. As electrons are transferred to the empty conduction band of the InAs layer leaving behind holes in the GaSb layer, electron and hole densities in the order of $\sim 10^{11}$ cm^{-2} can be obtained[65] without intentional doping or applying a gate voltage. This spatially separated 2D electron-hole system (2DEHS) is confined within different layers, and the 2D electron gas (2DES) and 2DHS are in equilibrium with each other at the interface. The energy gap between electron and hole subbands can then be tuned by varying the InAs/GaSb well width or by doping GaSb layers with Al to achieve semiconductor or semimetallic structure (effective band gap $E_g = -150$ to 300 meV).[66–68] This type of CQW system has several advantages. It is more desirable to produce exciton fluids at high densities, since the energy of the condensate would be larger, i.e., larger critical temperature, while optically pumped indirect exciton systems usually have lower exciton density ($\sim 10^{10}$ cm^{-2}).[41,49] The variation in the key properties with exciton densities can be systematically investigated by tuning the bias voltage with appropriate gates or the thickness of the GaSb cap layer[65] while high-power photoexcitation tends to drive the optically pumped exciton fluids into electron-hole plasma regime.[53] In addition, InAs/GsSb systems have potential applications for intersubband tunnel diodes[69] and mid-infrared (IR) optical devices.[70,71]

However, its advantages are also disadvantages. Excitons formed in equilibrium lead to difficulties in observation since they are dark excitons which do not luminesce. Fewer means are available for investigating the properties of these dark excitons. Though several types of transport property measurements have been proposed and carried out for exciton CQW,[33,72–74] the CQW samples were primarily investigated by optical means. One of the optical techniques for investigating these dark excitons is the cyclotron resonance (CR) spectroscopy by measuring magneto-IR absorption. However, while spatially resolved photoluminescence techniques[47–53] are used to investigate the macroscopic coherence of the photoexcited excitons, the spatially resolved IR technique has only been developed in the midinfrared range with a spatial resolution as good as microns.[75,76]

In this type of 2DEHS, several far-IR (FIR) active modes around CR have been observed and extensively studied in the past two decades. On one hand, the results suggest the formation of stable excitons by showing exciton's $1s$-$2p$ internal transitions;[66–68] on the other hand, they were interpreted as the hybridization gap due to a mixing of the electron and hole wave functions.[77–88] Though most of the FIR investigation reveal multiple modes around CR in InAs/GaSb CQWs, only a single mode was observed up to 12 T and interpreted as electron CR by Heitmann *et al.*[89] Earlier studies in InAs/GaSb superlattice systems show electron CR, intersubband transitions, and sometimes two absorptions near CR attributed to two occupied electron subbands.[90–94] More recent reports about the InAs/GaSb 2DEHS demonstrate results in favor of the hybridization interpretation.[87,88] The hybridization model in association with the $\mathbf{k} \cdot \mathbf{p}$ model can account for several features observed in this type of material, including the magnetic-field dependence of the CR energies,[79,87] oscillation in CR linewidth, mass, and amplitude,[66–68,83,89] the influence of a parallel magnetic field,[81,82,84,88] the slow decay rate of the temperature-dependent absorption intensity,[82,88] and the anomalies observed in magnetotransport measurements.[95–98]

In InAs/GaSb CQW systems, the overlap between the electron and hole subbands can be reduced or even completely eliminated by the confinement energy (small well width and high magnetic field); therefore minimizing the effect of the hybridization. It has been shown that the degree of hybridization can be modified by the width of InAs and GaSb well or by inserting a spacer layer.[64,82,83,86–88] Increasing InAs or GaSb well width tends to enhance the degree of hybridization by increasing the mixing of the electron and hole Landau levels (LLs), whereas the interposed barrier layer tends to reduce it. With a barrier layer as thin as 2–4 atomic layers, the mixing of the electron and hole wave functions can be suppressed,[27] because the penetration length should be on the order of 1 nm in this system.[83] Although the electron-hole Coulomb interaction decreases with increasing average distance between 2DES and 2DHS as the barrier layer is inserted, such a thin barrier layer has a negligible effect on the interlayer Coulomb interactions.[27] Generally, multiple absorption modes near CR were found in systems, which have configurations in favor of hybridization model in contrast to a single absorption mode, attributed to electron CR, which was observed in the weakly hybridized systems.[82,83,87]

In this paper, we present the result of the FIR magneto-optical study on weakly hybridized InAs/AlSb/GaSb CQWs, which have narrow well width and a 1 nm AlSb barrier layer separating electron and hole layers. This particular configu-
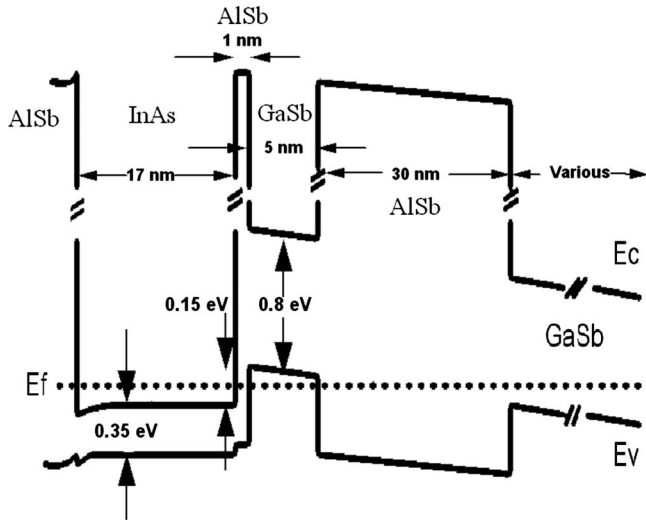
FIG. 1. Band diagram for the active region of the InAs-AlSb-GaSb heterostructure. E_C and E_V are the respective conduction-band minimum and top of the valence band in the GaSb cap layer. E_f marks the position of the Fermi level.
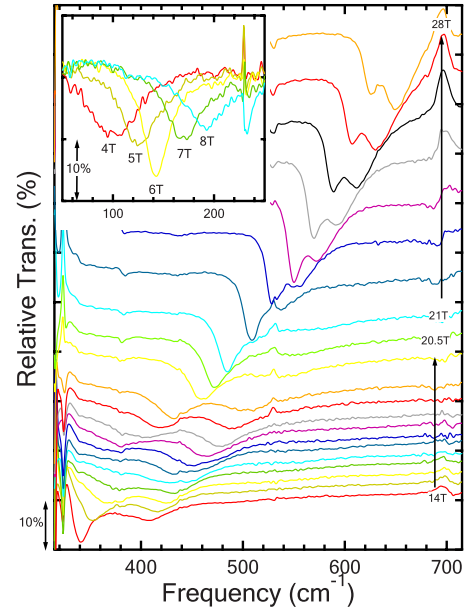

FIG. 2. (Color online) Magneto-FIR spectra from 14 to 28 T are displayed. The spectra are vertically shifted to demonstrate the evolution of the absorption modes with increasing magnetic field. Inset: spectra measured at low magnetic fields (4–8 T) are displayed and only a single absorption mode can be observed.

ration has been shown theoretically to have negligible hybridization coupling, but sufficient interlayer Coulomb coupling, and proposed as a candidate for achieving a stable condensed phase of excitons.[27] We have observed a pair of FIR absorptions occurring only at magnetic fields higher than 14 T with a field-independent (piecewise) energy separation. This pair of modes does not decay with increasing temperature up to 45 K and is insensitive to increasing parallel magnetic fields. These features distinguish our results from the ones reported in the literature. The connection between these phenomena and several models known to cause multiple absorption modes near CR is discussed. None of the models can account for the key features observed in this work, which suggests that more investigations should be carried out for this exciton system.

II. EXPERIMENTAL

The active region of the InAs-AlSb-GaSb CQW consists a 170 Å InAs quantum well (electron layer) and a 50 Å GaSb quantum well (hole layer), separated by a 10 Å AlSb barrier, and then completed by AlSb layers as outer barriers. The heterostructure's band diagram is shown in Fig. 1. The electron density is around 8.6×10^{11} cm^{-2} and the hole density is around 1.2×10^{11} cm^{-2} determined by the transport measurement[65] for the particular sample shown in this paper. The electron and hole densities can be determined separately from the Subnikov de Haas oscillations. This implies a very weak hybridization effect between the 2DES and 2DHS states. Samples whose electron densities ranging from 8×10^{11} to 9.5×10^{11} cm^{-2} and hole densities ranging from 1.2×10^{11} to 0.2×10^{11} cm^{-2} have been investigated. The carrier densities are controlled by the thickness of the GaSb cap layer and determined from the transport measurements fitted by two carrier conduction model.[99] The detail configuration of the heterostructure and its corresponding carrier

densities can be found in Ref. 65. The electron mobility is around 10^5 cm^2/V s.[65] The FIR transmission spectroscopy was carried out by a commercial Fourier transform interferometer up to 33 T from 4 to 45 K using light-pipe optics and a Si bolometer. The magneto-FIR modes are extracted by the ratio of the spectra measured with and without a magnetic field.

III. RESULTS AND DISCUSSION

A typical set of the magnetospectra measured within the range of values $14 \leq B \leq 28$ T is displayed in Fig. 2 and a pair of FIR active modes near the CR energy can be observed in the Faraday geometry. Below 10 T, only a single absorption mode is observed, attributed to the electron CR in the InAs QW, as shown in the inset of Fig. 2. From the CR energies at low magnetic fields, the effective mass is determined to be $0.037m_e$, consistent with the values reported in the literature, but much larger than the bulk electron mass $\sim 0.02m_e$. The observed absorption modes below and above the GaAs Restrahlen band exhibit an oscillation in CR amplitude, linewidth and masses, which is similar to the one reported in the literature.[66–68,89] All of these spectra are dark, which were taken without the beforehand light-emitting diode (LED) illumination. Unlike some reported results,[66–68,83] beforehand LED illumination does not induce new modes, nor does it change the CR energy or absorption intensity. Several works reported the observation of the hole CR in the GaSb layer and the hole effective mass was determined to be around $0.1–0.2m_e$.[67,78] No signs of hole CR have been observed beyond the noise level in any of the samples investigated, though high magnetic fields used in these measure-

ments can place the hole CR in the observable frequency range in our setups.

This result is similar to the general behavior of the reported multiple absorption modes. A pair of modes (in some reports, more than two modes), separated by a few millielectron volts, occurs near CR energy and their relative strength evolves with an increasing magnetic field. In this work, the lower-energy transition (CRL) is the strongest of the two at 14 T. With increasing magnetic field, the higher-energy transition (CRH) increases in intensity at the expense of CRL. This process is reversed at around 17 T, above which CRL increases in intensity at the expense of CRH. The process is then reversed again at around 23 T and CRH remains the dominating transition up to 33 T, which is the highest field measured for this series of samples. The evolution of the relative intensity is more similar to previous works, which interpreted the pair of modes in terms of CR and exciton's internal transitions;[66–68] while others, which interpreted the multiple absorption modes in terms of hybridization of electron and hole wave functions, reported an evolution that a new mode appears from the lower-energy side, and replaces those that tail off to the higher-energy region.[87]

Although this pair of modes exhibit features similar to the ones reported in the literature, several key differences are difficult to explain by the previous models, hybridization of the electron-hole wave functions or exciton's internal transitions. These key differences will be discussed in the following sections.

A. Occurrence of the CR splitting

One may notice that we prefer to refer the pair of modes found in this work as "CR splitting," in place of the term, "multiple absorption modes near CR," since we believe that they are both a consequence of electron CR involved with a transition between two electron LLs. In the hybridization model, the absorption modes arose from transitions between two electronlike LLs and between a holelike and an electronlike LL; while in the exciton model, one of the modes is due to the electron CR and the other, from the $1s$-$2p$ internal transitions of an exciton. For those transitions, we will refer to them as multiple absorption modes near CR, though we will also use this term to describe our findings occasionally, since it is a more general term. In addition, we will also refer to the two models in abbreviated terms as "exciton model" and "hybridization model."

It has been argued that hybridization model, or conduction-valence LL mixing, has an insignificant effect at high and low fields,[79] while the CR splitting in this paper occur only at magnetic fields higher than 14 T. In the literature, multiple absorptions were observed throughout and within nearly entire magnetic-field range investigated.[66–68,77–88] One may argue that the magnetic-field range, where the CR splitting were observed in this paper, is in fact the "intermediate" field range, but it is very unlikely. It is essentially impossible to place an intermediate regime within the confines of the given system.

The hybridization model is about an antilevel crossing gap which occurs due to a resonance between electron and
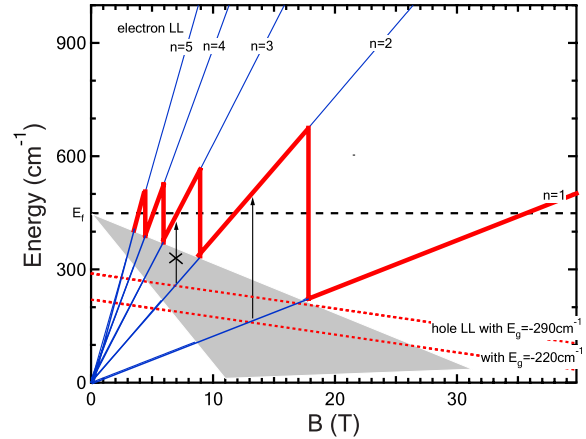

FIG. 3. (Color online) Electron (blue solid line; $n=1-5$) and hole (red dotted line; $n=1$) Landau-level structures vs magnetic field are plotted using the following parameters: $m_e^*=0.037m_e$, $m_h^*=0.1m_e$, and electron density $n_e=8.6\times10^{11}$ cm^{-2}. For convenience, energies are represented in per centimeter and g factors for both electron and hole levels are ignored. The Fermi-level oscillation is shown in a thick red solid line. The shaded area defines the region where the next set of LLs are below the FS. Two alternative values of the energy gap are discussed and shown in the two red dotted lines. CR splitting has been observed around $B=14$ T, and it coincides with the position of the antilevel crossing if $E_g=-220$ cm^{-1}, thus shown with an upward arrow. CR splitting was not observed around $B=7$ T, where an antilevel crossing is expected if $E_g=-290$ cm^{-1}, thus shown with the upward arrow crossed out. Higher hole LLs are ignored in this plot.

hole wave functions. It occurs at a magnetic field when the electron or hole LLs are aligned; in other words, at the points where the electron and hole LLs cross each other. Using electron mass $m_e^*=0.037m_e$, hole mass $m_h^*=0.1m_e$, and electron density as 8.6×10^{11} cm^{-2}, an energy diagram for the Landau levels in this system is established in Fig. 3. Near the crossing points, a transition between a holelike to an electronlike LL becomes possible due to the mixing of the electron and hole LL wave functions. As a result, more absorption modes make their appearance other than the transitions via two electron LLs. For the exciton model, the binding of electrons and holes requires the energy separation between them to be lower than the binding energy. We can expect anomalies as a result of electron-hole binding around these crossing points as well, though there should be a sizable excitonic binding energy before the alignment of the electron and hole LLs.[25]

By selecting a small effective band gap E_g ($\sim$220 cm^{-1}),[100] it can be clearly seen that any anomalies, due to either models, will not result in multiple absorption modes at low magnetic fields, since these anomalies are deep in the Fermi sea and the neighboring LLs are occupied. This explains why no CR splitting was observed at low magnetic fields in our samples or in the ones reported by Heitmann *et al.*[89] The electron densities in both cases are generally larger than the ones used in other reports, resulting in a larger Fermi energy E_f as compared to $|E_g|$.

At intermediate magnetic fields, anomalies near the crossing point ($\sim$14 T) can result in multiple absorptions through

LL transitions between the $n=1$ and $n=2$ electronlike LLs, and from the holelike LLs to the $n=2$ electronlike LLs, possibly responsible for the two broad modes observed between 14 and 18 T. However, CR splitting at higher magnetic fields cannot be a result of electron-hole LL mixing since electron LLs will no longer be aligned with the hole LLs at higher magnetic fields. This picture may explain why there exist two distinct regimes for CR splitting. In the intermediate magnetic-field regime (14–18 T), absorption modes are broad and weak with a larger energy separation, in which the hybridization may have an effect on these modes; while in the high magnetic-field regime ($B \geq 20$ T), absorption modes are sharp and strong with a smaller energy separation, in which hybridization has negligible effect.

Indeed, electron-hole LL mixing can occur at higher magnetic fields if the hole levels are located at higher energies. (i.e., larger $|E_g|$) A negative energy gap as large as -90 meV has been used to account for the multiple absorptions observed at high magnetic fields.[87] Even by shifting the hole LLs up by less than 10 meV, where the LL mixing can barely result in multiple absorptions at around 20 T, LL mixing will also result in additional absorption at around 7 T through LL transitions between $n=2$ and $n=3$ LLs, which were not observed in this series of samples. The position of the Fermi surface (FS) can place the minigap deep in the Fermi sea and naturally minimize the influence of the hybridization even if the sample is strongly hybridized. In fact, most of the reports in favor of the hybridization model have placed the FS between electron and hole subbands, i.e., within the energy gap, which will definitely result in multiple modes at very low magnetic fields.[77–85,87,88]

Another explanation for the lack of CR splitting at lower magnetic fields is that the interposed barrier layer suppresses the strength of the hybridization. No matter whether the FS is above the hole subbands or between the electron and hole subbands, hybridization in these samples is too weak to result in multiple modes even when the electron and hole LLs are aligned. The latter appears to be a more viable explanation since most of the band calculations place the FS within the band gap.

B. Energy separation of the splitting

The energy separation between the absorption modes appeared to be field independent when it was plotted over a wide range in previous reports. Multiple absorption modes were obtained from a set of spin-split LLs in the hybridization model. Although the magnetic-field-induced spin splitting may not be as significant as the antilevel crossing gap, the separation still carries a Zeeman term which grows with increasing magnetic field.[79] Upon taking a closer look at the data in the literature, the separation between the modes is indeed increasing with increasing magnetic field defined piecewise between the crossing points of the electron and hole LLs.[87,88] Since the region between two crossings expands with increasing magnetic field (see Fig. 3), a magnetic-field-dependent separation will be more pronounced at high magnetic fields.

To demonstrate that the separation between the CR splitting is field independent more precisely, the spectra were
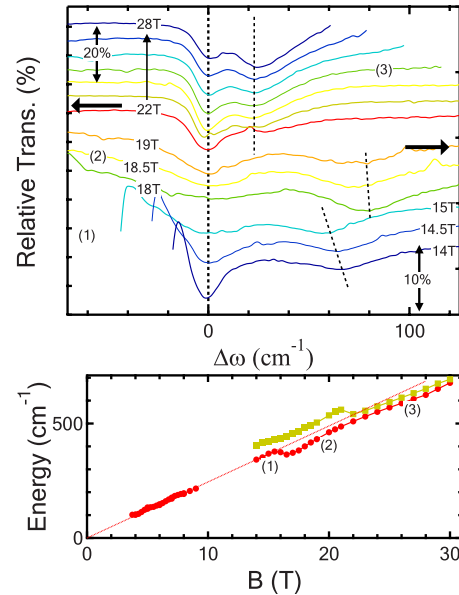

FIG. 4. (Color online) Top: to demonstrate the evolution of the energy separation between CRL and CRH more clearly, the spectra are horizontally offset to have CRL aligned. The part near the Reststrahlen band and the beamsplitter cutoff are removed for clarity. Bottom: the energies of the absorption modes as a function of magnetic field are displayed. CRL and CRH modes are represented in red circles and orange squares, respectively. The energy separation is about 60 cm^{-1} in zone (1), 80 cm^{-1} in zone (2), and 25 cm^{-1} in zone (3).

offset horizontally to align the CRL mode, as shown in Fig. 4 and the energies of the modes as a function of magnetic field are plotted at the bottom. In fact, there exist three zones with three distinct separation energies. In general, the energies of CRL and CRH increase linearly with increasing magnetic field. Two abrupt drops in each trace divide the region, where the CR splitting have been observed, into a succession of three zones, labeled: zones (1), (2), and (3), respectively. At the lower end of this region (zone 1), the separation energy is about 60 cm^{-1} before CRL makes an abrupt drop. The energy separation is then about 80 cm^{-1} (zone 2) until CRH also makes an abrupt drop in energy. Above 22 T, the separation is maintained at around 25 cm^{-1} (zone 3) as long as two modes are still observed up to 30 T. These values are of the same magnitude as compared to the exciton binding energies calculated by various works but none have suggested a field-dependent binding energy with discontinuities. The discontinuities in mode energies have been observed in several works.[67,68,87,88,101] These two abrupt drops in energy may be regarded as a part of the CR effective mass oscillation and it will be discussed in Sec. III E.

In zones (1) and (2), the energy separations between CRL and CRH are generally larger than the separation in zone (3), which is inconsistent with the concept that the CR splitting are a result of a pair of LLs with different spin states. Moreover, within zones (1) and (2), the energy separation is again slightly larger at lower fields, inconsistent with the nature of the Zeeman splitting. In zone (3), the energy separation maintains a nearly perfect field-independent energy separation up to 30 T. At high magnetic fields, the influence of the
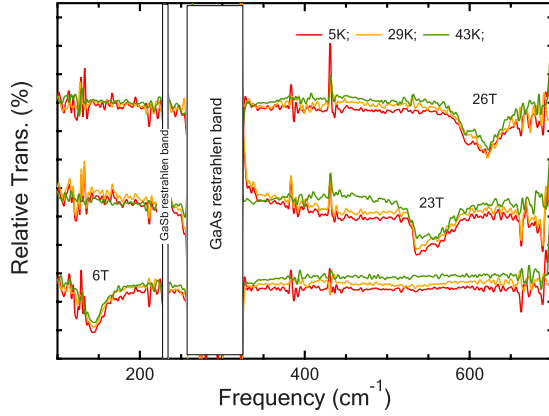
FIG. 5. (Color online) The temperature-dependent magneto-FIR spectra are displayed at three temperatures (5, 29, and 43 K) for three different magnetic fields. (6, 23, and 26 T) The spectra of different temperatures are slightly offset to make each trace more resolvable.

spin splitting should be discernibly visible. The lack of a magnetic-field-dependent energy separation in this work suggests that the CR splitting is not a consequence of a set of spin-split LLs, and is thus unlikely to result from the hybridization of the electron and hole wave functions. We here acknowledge that works in favor of the exciton model have reported an energy separation, which was also slightly larger at lower magnetic fields.[101]

C. Effect of the thermal excitation

Previous studies in these types of materials have revealed that multiple absorptions will merge into one if the temperature is sufficiently high.[67,68,82,88] In the exciton model, the higher-energy transition was interpreted as an exciton internal transition, while the thermal energy, overcoming the binding energy, breaks the bond between the electron and hole in the exciton.[67,68] Marlow *et al.*[82] then argued that the higher-energy transition did not decay fast enough for an exciton with a binding energy about 12 cm^{-1}; therefore, the decay of the higher-energy transition is a result of populating the higher-energy spin-split LLs with increasing temperature and interpreted it in terms of the hybridization model. Petchsingh *et al.*[88] then observed that multiple modes merged into one at around 40 K while the sum of the absorption intensity increases with increasing temperature. The increase in the integrated intensity has been interpreted to mean that the thermal excitations give access to transitions associated with levels away from the minigap with lower degree of hybridization.[88] In spite of how the temperature dependence was interpreted in the past, multiple modes converge at high temperatures and usually merged into one at even higher temperatures beyond the critical point of modal convergence.

A set of spectra measured at 6, 23, and 26 T for three different temperatures are displayed in Fig. 5 to demonstrate the temperature dependence of the CR splitting. One can instantly see that the absorption modes are insensitive to increasing temperature. These modes are rather robust against rising thermal excitations, which suggests that both modes

result from free-carrier excitations with the FS far away from the minigap, consistent with the picture illustrated in Sec. III A.

As indicated in Sec. III A, the minigap, if it existed, is deep in the Fermi sea and the states around minigaps are occupied. Since the FS is pinned at the corresponding electron LLs with a LL separation around several hundred Kelvin, thermal excitation at 40 K can hardly distort the FS at high magnetic fields. Though it is possible that the minigap lies closer to the FS at intermediate fields (14–18 T), the spectra at these fields are not displayed due to the reduced signal-to-noise ratio at higher temperatures. The broad peaks observed at intermediate fields are close to the noise level but the results are more likely to be temperature independent.

D. Effect of parallel field

The nature of the hybridization model is an antilevel crossing gap as a result of Pauli exclusion principle, creating minigaps near the resonances of electron and hole LL wave functions. A parallel magnetic field can cause a phase shift between electrons and holes, moving the electron and hole dispersion relations in opposite directions in *k* space.[84,102,103] This shift decouples the dispersion relations and eliminates the formation of the minigap. This phenomenon was experimentally confirmed in the InAs/GaSb CQWs,[81,82,84,88] and was considered as plausible evidence in support of the formation of minigaps in these types of materials. Similar to what happened to the absorption modes when the temperature is increased, multiple absorption modes merge into one with increasing parallel magnetic field;[80,82,84,88] while Petchsingh *et al.*[88] reported an increase in the integrated intensity occurred simultaneously not unlike the one discussed in the previous section. A parallel magnetic field as small as 7 T suppresses the hybridization and destroys the formation of the minigaps even in the strongly hybridized samples.[82]

The sample is placed on a wedge with the normal direction of the sample tilted at an angle from the direction of the magnetic field. The tilt angle was determined to be 33° by fitting the CR energies at low magnetic fields. A set of magneto-FIR spectra measured in the tilted geometry is displayed in Fig. 6 and the energies of the CRL and CRH modes as a function of the total magnetic field are displayed in the bottom. The magnitudes of the parallel (B_{par}) and perpendicular (B_{per}) fields are shown in the bracket and a parallel magnetic field as large as 18 T has been reached. The spectra were divided into two groups; the spectra with a perpendicular field larger than 20 T are displayed in the top graph while the ones below 20 T are displayed in the bottom. Twenty tesla was the magnitude of the magnetic field which divided the CR splitting into a sharp-peak region and a broad-peak region in the Faraday geometry.

As compared to the spectra measured in the Faraday geometry, the absorption modes become sharp and strong at around the same total magnetic field, instead of the same perpendicular field, suggesting that the sharp-peak behavior, or the narrowing of the linewidth, are induced by the total field, independent of the tilt angles. However, the abrupt drops of mode energies occur at around the same perpen-
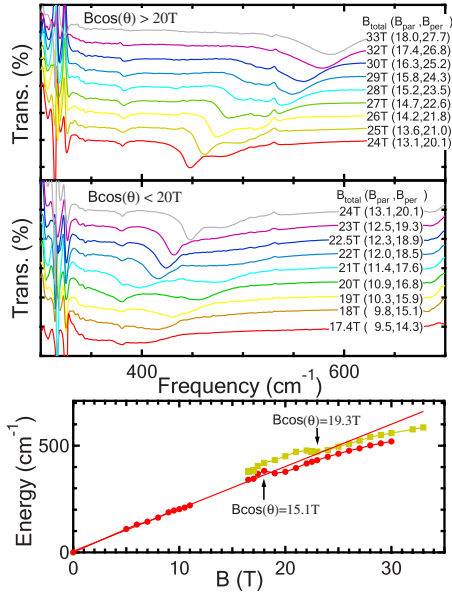
FIG. 6. (Color online) Top: magneto-FIR spectra measured in tilted geometry (33°) from 17.4 to 33 T are displayed. The spectra are divided into two groups based on the strength of the perpendicular magnetic field. The magnitudes of the parallel (B_{par}) and perpendicular (B_{per}) fields at a given total field (B_{total}) are shown by the values in the bracket. Bottom: the energies of the absorption modes as a function of magnetic field are displayed. CRL modes are shown in red circles and CRH modes are shown in orange squares. The energy separation is about 40 cm^{-1} in zone (1), 75 cm^{-1} in zone (2), and 36 cm^{-1} in zone (3).

dicular fields; in other words, they occur at the same filling factors or the same LL separations.

The CR splitting are observed at a parallel magnetic field higher than 10 T while it was shown to be sufficient to suppress the formation of the minigaps in strongly hybridized samples.[84,88] By comparing the spectra of similar perpendicular fields, but different parallel fields, CRH in comparison to CRL becomes slightly stronger, which can simply be a result that their relative strength are mainly determined by the total field, instead of the perpendicular field.

The energies of CRL and CRH generally scale with tilting angle θ as cos θ with an additional suppression at high fields, possibly due to the additional confinement introduced by the high parallel fields. Additional confinement reduces the effective well width, thus resulting in a larger effective mass; in other words, a lower CR energy. The energy separation is about 40 cm^{-1} in zone (1), 75 cm^{-1} in zone (2), and 36 cm^{-1} in zone (3). The first two are slightly smaller than their counterparts in the Faraday geometry while the last one is slightly larger than its counterpart. The energy separation is slightly smaller at intermediate magnetic fields, which may be due to the closing of the minigaps by increasing parallel magnetic field; however, it also implies that the effect of the hybridization is secondary to the major factor causing the CR splitting. At high magnetic fields, the separation becomes larger, which cannot be explained by the hybridization model, or the concept of spin-split electron CR.

In the tilted geometry, parallel magnetic field can also cause the LLs of different electron subbands to couple,

known as resonant subband LL coupling.[104] A quick estimate places the electron's second subband 105 meV above the first, which is too high to produce an effect in measurements below 33 T.

E. Oscillation of CR amplitude, linewidth, and effective mass

The oscillation of CR was found to be more pronounced in the InAs-based 2DS (Refs. [66], [68], [89], [105], and [106]) than the one in the GaAs-based systems.[107] On one hand, CR linewidth maxima were observed at even filling factor ν's and the minima at odd ν's,[66,68,89] which was attributed to the ν-dependent screening of impurity scattering by the 2D electron gas.[108–110] On the contrary, linewidth maxima were observed for odd ν's in the spin-resolved CR measurements,[105,106] which was attributed to the nonparabolicity effect.[111] The driving mechanism behind such a pronounced CR oscillation particularly in the InAs-based 2DS is not fully understood; nonetheless, CR oscillation can still be used to reveal principal parameters, such as carrier densities, which in this case, help to determine which mode, CRL or CRH, is more likely to result from the typical electron CR.

Unlike the multiple absorption modes reported in the literature, the observed CR splitting is insensitive to increasing temperature or parallel magnetic fields. As a result, both of them can be a conventional electron CR. To understand the origin of the CR splitting, it is very important to identify which one results from the typical electron CR. An electron-hole coupling is likely to have an attractive interaction, which tends to result in an absorption at higher energies as more energy is needed to break the coupling; while an electron-electron coupling is likely to have a repulsive interaction, leading to an absorption mode at lower energies.

The oscillations of CR effective mass, amplitude, and linewidth (half width at half maximum) are displayed in Fig. 7. At low fields, the period of the oscillation agrees well with the electron density of 7.4×10^{11} cm^{-2} with linewidth maxima for even-valued filling factor ν's. This result is consistent with the oscillation observed in the InAs QW and InAs/GaSb CQW for the electron CR.[66,68,89] By using the CR oscillation observed at lower magnetic fields, one can extend the oscillations to higher magnetic fields and the oscillation pattern of CRL mode is consistent to the oscillation pattern of the CR observed at low fields. Therefore, we believe that the CRL mode results from the conventional electron CR in the InAs layer while CRH is a mode induced by the unique condition in the InAs/GaSb CQW. Since it has produced an additional mode at a higher energy, the nature of the coupling is likely to be attractive. Electron-hole interaction is one of the likely causes, whereas the hybridization results from the antilevel crossing of the LLs, arising from the repulsive interactions between the states. In the works supporting the hybridization model, a new mode emerges from the lower energy side,[87] which illustrates that the interaction is repulsive.

The CRL's effective mass oscillates with the filling factor and a sudden rise in the effective mass occurs at around $\nu \sim 2$, corresponding to the abrupt drop in CRL energy in Fig. 4; then, it is possibly approaching another effective-mass
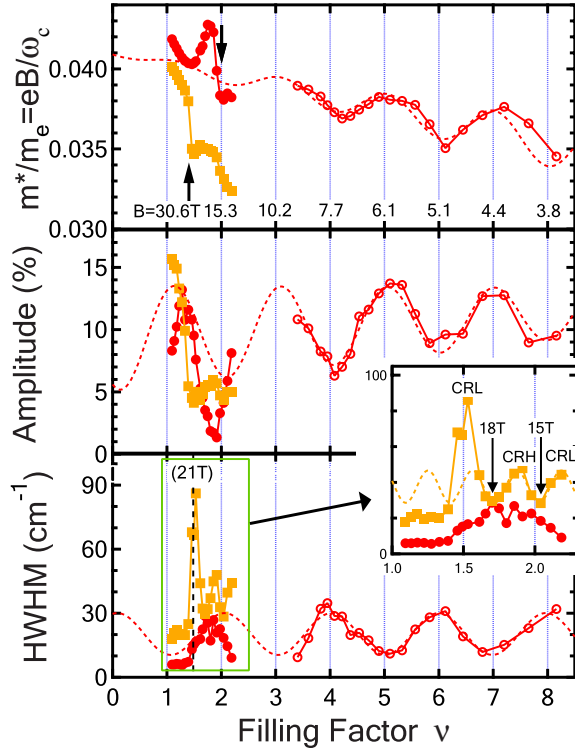
FIG. 7. (Color online) The oscillation of effective mass, amplitude, and linewidth for CRL (red open circles for lower fields, where only one absorption mode was observed and red filled circles for higher fields) and CRH (orange filled squares) as a function of filling factor is plotted. The red dash lines are used as guides for extending the oscillation to the high field. The sudden rises in the CR effective mass for CRL and CRH modes are indicated by a downward and an upward arrow, respectively. From the CR oscillation, the electron density was determined to be 7.4×10^{11} cm^{-2}. Inset: expanded view of the linewidth oscillation at high magnetic fields.

maximum near $\nu \sim 1$. The sudden rise in effective mass may be related to the unique properties of the $\nu=2$ quantum-Hall states, which has been a subject of interest recently.[112] Discontinuities in CR energy and thus jumps in CR effective mass have been observed in InAs/GaSb CQW,[66,68,83,85,87,88] and the effective-mass minima or jumps were found to be associated with even-valued filling factor ν's.[66,68]

Though the region where the CRH mode can be observed is too narrow to show significant periodic behavior, a similar effective-mass jump has been observed at around 21 T, appearing as if it is offset from the CRL's oscillation. The induced CR-like mode in InAs/GaSb CQW was also found to exhibit an oscillation pattern, which is offset from the oscillation the electron CR oscillation.[67,68] Both of these jumps are filling factor or perpendicular field dependent as shown in Sec. III D. One can hardly correlate the two effective jumps ($\nu=1.5$ and 2) to one another and in terms of filling factors, $\nu=1.5$ does not have any physical significance. The effective-mass jump may also occur at around $\nu=2$ but from a region of slightly higher carrier density; therefore, CRH's oscillation appears as if it is offset from CRL oscillation. The implication of this concept will be discussed in Sec. IV C.

The amplitude oscillation at high magnetic fields, i.e., lower filling factors, is more driven by the exchange of the integrated intensity between the CR splitting. CRL's amplitude decreases while CRH's increases between $14 < B < 17$ T, then the process is reversed between $17 < B < 21$ T. Both amplitudes increase with increasing magnetic field between $21 < B < 23$ T, corresponding to an anomalous linewidth narrowing at 21 T (transition from the broad-peak to the sharp-peak regions). In the end, CRH's amplitude continues to increase for $B \geq 23$ T while CRL's amplitude decreases with increasing magnetic fields. The evolution of the CR amplitudes tends to mimic the evolutionary profile of the absorption strength observed in Fig. 2.

The linewidth oscillation of CRL and CRH at high magnetic fields are expanded in the inset, which displays an interesting pattern. While CRL's linewidth generally oscillates with the filling factors at high magnetic fields, CRH's oscillates at a much faster rate. If this rate is taken seriously, such a fast oscillation corresponds to an electron density as large as 4.75×10^{12} cm^{-2} with linewidth maxima at even filling factors (10, 12, and 14) and minima at odd filling factors (9, 11, and 13), opposite to the CRL's linewidth oscillations. It is very unlikely that such a dense region (by an order) is formed in this system. The maxima of the CRH's linewidth corresponds to the fields, where one of the two modes is dominating, while the two minima correspond to the fields where the two modes are of nearly equal strength. It suggests that the linewidth oscillation for CRH mode is also strongly affected by the intensity exchange between the CR splitting.

At around 21 T, linewidths of both modes collapse, though it is less significant for CRL, since its linewidth is decreasing from $\nu=2$ to $\nu=1$. At very high fields ($B \geq 23$ T), both linewidths remain small and become independent of the magnetic fields or filling factors. The sharp reduction in photoluminescence linewidth was attributed to a phase transition of the exciton system into an ordered state.[41] This sharp reduction in CR linewidth could be an effect parallel to that found by Fukazawa *et al.*, but we lack the evidence supporting that a critical temperature T_C is associated with the narrowing of the CR linewidth. The CR splitting appears to be temperature independent up to 43 K and it is the highest temperature attainable with our present high-field probe.

IV. DISCUSSION

Many aspects of this work have been discussed and compared with the two most widely used models, the exciton model and the hybridization model. As indicated in the previous sections, neither one can account for the features found in this paper. Though they appear to be quite different, interlayer Coulomb interaction and hybridization of electron-hole wave functions share many similar properties. By considering the electron-hole system's Hamiltonian as a simple 2 $\times 2$ matrix as illustrated by Petchsingh *et al.*,[87] hybridization effect and interlayer Coulomb interaction will both appear in the off-diagonal term, thus resulting in similar types of energy characteristics, though an interlayer Coulomb interaction is possibly more complicated. The hybridization model

is realized as two intercepting dispersion relations; one belongs to the electron and the other to the holes. The minigaps are formed at the intercepts of the electron and hole dispersion relations. Coulomb interactions, in the form of $1/k^2$, should also have a prominent effect at the intercepts. When the hybridization model is realized in an energy diagram shown in Fig. 3, a minigap of several millielectron volts is formed when the electron and hole LLs are aligned with increasing magnetic field. By contrast, an exciton is formed with a characteristic energy of several millielectron volts when the single-particle energy gap becomes smaller than the binding energy, i.e., when the electron and hole LLs are nearly aligned. For the hybridization model, the $\mathbf{k} \cdot \mathbf{p}$ model has established an energy diagram for the multiple absorption modes that agree well with the observed mode energies, which may also reflect what is going to occur if the interlayer Coulomb interaction is included in the $\mathbf{k} \cdot \mathbf{p}$ model.

A. A modified exciton model

We would like to suggest a small tweak to the original exciton model. As indicated in Sec. III E, the CRL mode is likely to result from the conventional electron CR, which is a LL transition from $n=0$ to $n=1$. Instead of having exciton internal transitions, CRH is an exciton pair-breaking excitation. The exciton absorbs the photon energy, breaking the electron-hole pair and the electron makes a LL transition from $n=0$ to $n=1$ LL. As a result, its magnetic-field dependence is similar to the electron-LL transition but is instead offset by the binding energy. Since the spin-split ground-state LL is fully occupied up to 30 T, a pair broken by the thermal excitations cannot place the electron back to the ground state, thus rendering it forbidden. Extra thermal energy is needed in order to break the pair and place the electron in the next available LL, which is separated by about 200 cm^{-1} (25 T with $g \sim -8$). As a result, both modes are insensitive to the temperature changes up to 43 K within the magnetic-field range investigated. Unfortunately, this concept suffers a severe setback since the hole density is much smaller than the electron density. Even if each hole is bound to an electron, the CRH mode should remain the weaker mode of the two; which contradicts observation unless, we assume that a hole is bound with several electrons forming the many-particle state, which release an electron after it absorbs the photon energy.

B. Spin-split CR

As indicated in Sec. III A, the hybridization model cannot account for the CR splitting observed at high magnetic fields, or it will result in multiple absorption modes at low fields. It does not seem to rule out the possibility that the CR splitting are caused by the spin-split LLs as a result of a difference in the g factors of LLs with different LL index; in this case, $n=1$ and $n=2$ LLs. We have basically ruled out the spin-split CR as a possible cause for the CR splitting when we ruled out the hybridization model since it also arose from a set of spin-split LLs. At this juncture, we will discuss several additional discrepancies between the observed features and the

features that is expected if the CR splitting are a result of the spin-split LLs.

In the single-particle picture, such an effect is basically the Zeeman splitting, which increases linearly with increasing magnetic field as $\Delta g \cdot \mu_B \cdot B$, where Δg is the difference in the g factor and μ_B the Bohr magneton. The observed energy separation is field independent at high magnetic fields while being slightly larger at lower magnetic fields. To account for the observed energy separation, Δg needs to be rather complicated, which has to be field dependent as $1/B$ at high fields, and as $1/B^\gamma$ with $\gamma > 1$ piecewise defined at the intermediate fields. Additionally, this must occur between $\nu \gtrsim 2$ and $\nu = 1$.

The line shapes of the CR splitting are not symmetrical since CRH mode always has a larger linewidth. This would require the system to have a spin-direction-selective scattering mechanism. The strength of the two modes are nearly equal for three different fields, which are 15.5 T, 19 T, and 25 T, respectively. The spin-split CR should have nearly equal contributions at $\nu \sim 2$ and then one of them, usually the lower-energy transition, increases at the expense of the other one with increasing magnetic field. The intensity of the two modes of the CR splitting exchange several times between $\nu = 2$ and $\nu = 1$ and there is no way to account for all three magnetic fields, where the intensity of the two modes are nearly equal to each other. The CR splitting should start to appear at around $\nu = 4$, which is around 8 T with at least three different transition energies. One is at around the typical CR energy if the $n=2$ and $n=3$ LLs have the same g factor and a pair of modes offset by $\pm \Delta g \cdot \mu_B \cdot B$. Such splitting has not been observed in this system. In addition, the features observed when the sample is tilted are also against the spin split CR; in particular, the energy separation increases with increasing tilt angle θ while it should be tilt-angle independent for spin splitting.

C. Spontaneous phase separation

It has been discussed in Sec. III E that CRH's oscillation appears to be offset from CRL's oscillations with the CR effective-mass jump at 21 T. It is reasonable to assume that the CRH's oscillation offset results from regions of slightly higher electron density. As a result, CRH mode is essentially an electron CR mode and inherit the properties of the electron CR in InAs layer. By assigning the CRH's effective-mass jump at 21 T to $\nu = 2$, one can deduce a carrier density of around 10.2×10^{11} cm^{-2} for these regions. Other assignments are unlikely because the carrier density for CRH regions will be too high.

The assignment of CRH's effective-mass jump to $\nu = 4$ or larger even integers will result in several features which are inconsistent with the experimental results. Since the integrated intensity of a CR mode generally increases with increasing electron density, CRH's intensity should be much larger than CRL's. More CR oscillation cycles should have been observed in the investigated magnetic-field range. Finally, higher carrier density will lead to some features, which are inconsistent with the model we are about to propose.

We propose that a spontaneous phase separation is induced by increasing magnetic field and the 2DES splits into

two phases: puddles with the electron density of around 10.2×10^{11} cm^{-2} surrounded by the region with the electron density of around 7.4×10^{11} cm^{-2}. Such an idea has been discussed for the type-II bosons, i.e., excitons.[20,113] The formation of the puddles requires a degree of additional lateral confinement to pool the electrons into puddles. It has been proposed that electrons were trapped by the localized states on the surface[114–116] or in puddles between repulsive scatterers,[117] in which the CR energy of the weakly bound electrons in the harmonic traps is shifted to a value $\omega^2 = \omega_c^2 + \Omega^2$, where Ω is related to the curvature of the confining potential. As a result, both of the CR and the confinement shifted CR increase linearly with increasing magnetic field at sufficiently high magnetic fields, as if the latter mode offsets from the former mode by a constant energy separation. Moreover, the energy separation between the two, ω_c and ω, will be larger at lower magnetic fields, but nearly a constant at high magnetic fields. Both of these features qualitatively agree with the experimental results and the latter feature cannot be explained in term of the hybridization model.

A quantitative description for the CRH energies will be difficult because the electron CR energy in InAs 2DES oscillates with filling factor[66,68,85,87–89] and is affected by the nonparabolicity effect in InAs. In order to find the confinement shifted CR energy (CRH), we will first establish a base line for the electron CR energy (CRL) at high fields by linearly fitting the CR energy below and above $\nu = 2$ using two field-independent effective masses. The CR energy for CRL mode can be well described by $m^* = 0.038 m_e$ for $\nu > 2$ and $m^* = 0.041 m_e$ for $\nu \leq 2$. CRL's energy can then be described as shown in the inset of Fig. 8. Then, CRH's energy can be fitted by the quadratic sum based on its corresponding filling factor. As shown in the inset of Fig. 8, the CRH energy can be well described with the parameter $\Omega \sim 200$ cm^{-1}.

The formation of the puddles can also account for several less pronounced features. The linewidth of CRH mode is always larger than CRL mode, which has been used as evidence against the idea of the spin-split CR. Either the edge scattering arising from the puddle-environment interface or the variation in the puddle sizes can contribute to the broadening of the linewidth. The linewidth of CRH mode is unusually large at around 21 T, reaching a value of 100 cm^{-1}. Due to the variation in puddles' electron densities, puddles of different carrier density will go through their $\nu = 2$ effective-mass jump at different fields. The CR energies from the puddles of lower electron densities will drop before others, thus smearing out the CRH mode.

Most importantly, this concept can also account for the exchange of the integrated intensity from 14 T ($\nu \gtrsim 2$) to 30 T ($\nu \sim 1$), which will be difficult to explain in terms of the Fermi-surface oscillation. Energy diagrams for the LLs in the puddles (CRH) and in the environment (CRL) are plotted in Fig. 8 in order to illustrate the exchange of the electrons, leading to the exchange of the integrated intensity. The vertical lines separating the CRL's and CRH's LLs represent the puddle-environment interface. These energy diagrams are plotted for four particular magnetic fields, indicated by the values shown on top of the vertical lines. The energies of the LL are plotted to scale based on the measured energies of CRL and CRH modes at different magnetic fields. The spin
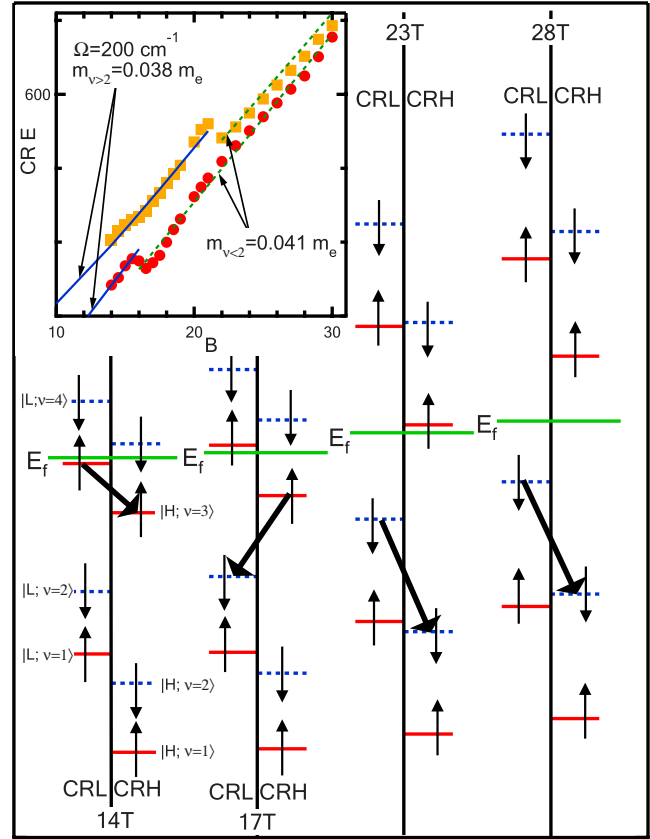

FIG. 8. (Color online) Energy diagram of the LLs in the puddles (CRH) and in the environment (CRL). The energies of the CRH LLs are shifted by about -200 cm^{-1} to account for an energy trap for the electrons, resulting in the difference in the electron densities. The thick vertical lines represent the interfaces between them and the energies of the LL are plotted to scale based on the measured energies of CRL and CRH modes. To distinguish the spin-up (red solid line) and spin-down (blue dashed line) LLs, a g factor of -8 is used to calculate the Zeeman splitting. The positions of the FS at different fields are represented in green solid lines and the bold arrows show the direction of the electron transfer. Inset: the energies of the CRL and CRH modes are fitted by a phenomenological model, in which the CR oscillation is ignored and the effective-mass jump near $\nu = 2$ is approximated by a step function. When $\nu > 2$ (blue solid lines), the electron effective mass is $0.038 m_e$ and $0.041 m_e$ when $\nu \leq 2$ (green dotted lines). With $\Omega = 200$ cm^{-1}, the energies of CRL and CRH mode can be fitted by the magnetic-field dependence of the electron CR and the confinement shifted CR, respectively.

states of the LLs are indicated by the vertical arrows and styles of the lines representing the LLs. A g factor of -8 is applied[64] to distinguish LLs of different spin states. For convenience, the LLs will be labeled by the filling factor instead of the LL index and the spin state. Each LL will be labeled as $|H$ or $L; \nu\rangle$, in which the first term indicates whether it is a LL in the puddles (H) or in the environment (L).

The LLs in puddles (CRH) are offset by -200 cm^{-1} to represent an energy trap for electrons, creating a difference in the electron densities between the two regions. With increasing magnetic field, LLs in the puddles and in the environment will take turn to pass the FS, resulting in the ex-

change of the electrons between the two regions and thus the exchange of the integrated intensity between the two modes. The bold arrows indicate the direction of the electron flow with increasing magnetic field until the magnetic field reaches the magnetic field of the next energy diagram to its right.

Starting from the 14 T energy diagram, the electrons fill LLs up to the $|L; 3\rangle$ LL. With increasing magnetic field, the degeneracy of the LLs increases. Some electrons in the $|L; 3\rangle$ LL should move across the interface to fill the unoccupied states in the $|H; 3\rangle$ LL, when the empty states become available. As the environment (CRL) loses electrons to the puddles (CRH), the integrated intensity of the CRH mode increases at the expense of the CRL mode.

The transfer of the integrated intensity is reversed at around 17 T. The $|L; 3\rangle$ LL now passes the FS and the electrons are filling up to the $|H; 3\rangle$ LL. With increasing magnetic field, the degeneracy of the LLs increases. Some electrons in the $|H; 3\rangle$ LL should move across the interface to fill the unoccupied states in the $|L; 2\rangle$ LL, when empty states become available. As the puddles (CRH) lose electrons to the environment (CRL), the integrated intensity of the CRL mode increases at the expense of the CRH mode.

Likewise, the transfer of the integrated intensity is reversed again at around 23 T when the $|H; 3\rangle$ LL passes the FS and the electrons fill up to the $|L; 2\rangle$ LL. The electron flow is directed to the puddles again and the integrated intensity of the CRH mode increases with increasing magnetic field.

The size of the puddles can be estimated based on the equation proposed by Mikeska *et al.*[114] If the depth of the trap is around 200 cm^{-1}, the average diameter of the puddles is about 250 Å. The temperature dependence of the CR splitting can be easily explained if the triple point of the phase separation is much higher than 40 K. Other than some exotic origins such as the collective ground states resulting from the exciton BEC,[20,113] a more conventional possibility involves the holes in the GaSb layer, which trap the electrons into puddles through the interlayer Coulomb interaction. A quick estimate for the depth of the electron trap yields a value in the appropriate range provided the band bending and the in-plane screening are ignored. Kallin and Halperin[118] had previously discussed an impurity mode induced by the impurity scattering; while, in this case, the impurities are the holes on the other side of the barrier.

V. SUMMARY

InAs/GaSb-based type II and broken-gap quantum wells have been extensively studied in the past as a promising candidate for finding BEC of excitons in bilayer 2DS without photoexcitation. The works in the past have revealed multiple absorption modes near CR which were interpreted in two different models. On one hand, these modes indicated the formation of stable exciton phase, which exhibits an additional mode at the exciton's 1*s*-2*p* internal transitions. On the other hand, these modes seem to result from the formation of the minigaps due the hybridization of the electron and hole wave functions. Recent studies in these types of materials have been strongly in favor of the hybridization model.

We have studied a series of weakly hybridized InAs/AlSb/ GaSb CQWs, in which the hybridization effect is minimal by having narrower well width and an AlSb barrier interposed between InAs and GaSb layers. We have observed a pair of modes, only at magnetic fields higher than 14 T, in this series of samples; whereas, only a single absorption mode, attributed to electron CR, was found in the weakly hybridized samples in the past.

The CR splitting exhibit several features, which are very different from those reported in the past. The energy separation is slightly larger at lower magnetic field while it is magnetic-field independent at high magnetic field. The CR splitting was robust against increasing thermal excitations and increasing parallel magnetic fields. These key differences are inconsistent with the two models proposed in the past.

Several ideas have been proposed and discussed in this paper. The concept, of spontaneous phase separation, seems to account for most of the features observed in this work. The phase separation can be a result of an electron trap: a consequence of the interlayer Coulomb interaction from the holes in the GaSb layer, which shows that the electron-hole interaction played a vital role in this system.

[1] J. Bardeen, L. N. Cooper, and J. R. Schrieffer, Phys. Rev. **108**, 1175 (1957).

[2] J. M. Blatt, K. W. Böer, and W. Brandt, Phys. Rev. **126**, 1691 (1962).

[3] L. V. Keldish and Y. V. Kopaev, Sov. Phys. Solid State **6**, 2219 (1965).

[4] A. N. Kozlov and L. A. Maximov, Sov. Phys. JETP **21**, 790 (1965).

[5] L. V. Keldish and A. N. Kozlov, Sov. Phys. JETP **27**, 521 (1968).

[6] D. Jérome, T. M. Rice, and W. Kohn, Phys. Rev. **158**, 462 (1967).

[7] S. Nakajima and D. Yoshioka, J. Phys. Soc. Jpn. **40**, 328 (1976).

[8] B. A. Volkov, Yu. V. Kopaev, and A. I. Rusinov, Sov. Phys. JETP **41**, 952 (1976); **43**, 589 (1976).

[9] E. Fenton, Phys. Rev. **170**, 816 (1968).

[10] A. V. Korolev and M. A. Liberman, Phys. Rev. B **47**, 14318 (1993).

[11] S. I. Shevchenko, Phys. Rev. Lett. **72**, 3242 (1994).

[12] A. V. Korolev and M. A. Liberman, Phys. Rev. Lett. **72**, 270 (1994).

[13] L. Balents and C. M. Varma, Phys. Rev. Lett. **84**, 1264 (2000).

[14] Y. E. Lozovik and V. I. Yudson, JETP Lett. **22**, 274 (1975).

[15] D. Yoshioka and H. Fukuyama, J. Phys. Soc. Jpn. **45**, 137 (1978).

[16] I. V. Lerner and Y. E. Lozovik, J. Phys. C **12**, L501 (1979).

[17] G. Bastard, E. E. Mendez, L. L. Chang, and L. Esaki, Phys. Rev. B **26**, 1974 (1982).

[18] Y. A. Bychkov and E. I. Rashba, Solid State Commun. **48**, 399 (1983).

[19] S. Datta, M. R. Melloch, and R. L. Gunshor, Phys. Rev. B **32**, 2607 (1985).

[20] D. Paquet, T. M. Rice, and K. Ueda, Phys. Rev. B **32**, 5208 (1985).

[21] X. Zhu, J. J. Quinn, and G. Gumbs, Solid State Commun. **75**, 595 (1990).

[22] D. Yoshioka and A. MacDonald, J. Phys. Soc. Jpn. **59**, 4211 (1990).

[23] G. E. W. Bauer, Phys. Rev. Lett. **64**, 60 (1990).

[24] X. M. Chen and J. J. Quinn, Phys. Rev. Lett. **67**, 895 (1991).

[25] X. X. Xia, X. M. Chen, and J. J. Quinn, Phys. Rev. B **46**, 7212 (1992).

[26] Y. Naveh and B. Laikhtman, Phys. Rev. B **49**, 16829(R) (1994).

[27] Y. Naveh and B. Laikhtman, Phys. Rev. Lett. **77**, 900 (1996).

[28] X. Zhu, P. B. Littlewood, M. S. Hybertsen, and T. M. Rice, Phys. Rev. Lett. **74**, 1633 (1995).

[29] H. Chu and Y. C. Chang, Europhys. Lett. **35**, 535 (1996).

[30] S. de-Leon and B. Laikhtman, Phys. Rev. B **61**, 2874 (2000).

[31] S. De Palo, F. Rapisarda, and G. Senatore, Phys. Rev. Lett. **88**, 206401 (2002).

[32] A. V. Balatsky, Y. N. Joglekar, and P. B. Littlewood, Phys. Rev. Lett. **93**, 266801 (2004).

[33] J. P. Eisenstein and A. H. MacDonald, Nature (London) **432**, 691 (2004).

[34] B. Laikhtman and L. D. Shvartsman, Phys. Rev. B **72**, 245333 (2005).

[35] Y. Lozovik, I. Kurbakov, and M. Willander, Phys. Lett. A **366**, 487 (2007).

[36] V. B. Timofeev, V. D. Kulakovskii, and I. V. Kukushkin, Physica B **117–118**, 327 (1983).

[37] N. Peyghambarian, L. L. Chase, and A. Mysyrowicz, Phys. Rev. B **27**, 2325 (1983).

[38] D. Snoke, J. P. Wolfe, and A. Mysyrowicz, Phys. Rev. Lett. **59**, 827 (1987).

[39] E. Fortin, S. Fafard, and A. Mysyrowicz, Phys. Rev. Lett. **70**, 3951 (1993).

[40] D. P. Young, D. Hall, M. E. Torelli, Z. Fisk, J. L. Sarrao, J. D. Thompson, H.-R. Ott, S. B. Oseroff, R. G. Goodrich, and R. Zysler, Nature (London) **397**, 412 (1999).

[41] T. Fukuzawa, E. E. Mendez, and J. M. Hong, Phys. Rev. Lett. **64**, 3066 (1990).

[42] U. Sivan, P. M. Solomon, and H. Shtrikman, Phys. Rev. Lett. **68**, 1196 (1992).

[43] B. E. Kane, J. P. Eisenstein, W. Wegscheider, L. N. Pfeiffer, and K. W. West, Appl. Phys. Lett. **65**, 3266 (1994).

[44] V. L. Berezskii, Sov. Phys. JETP **34**, 610 (1971).

[45] J. M. Kosterlitz and D. J. Thouless, J. Phys. C **6**, 1181 (1973).

[46] J. E. Golub, K. Kash, J. P. Harbison, and L. T. Florez, Phys. Rev. B **41**, 8564(R) (1990).

[47] L. V. Butov, A. L. Ivanov, A. Imamoglu, P. B. Littlewood, A. A. Shashkin, V. T. Dolgopolov, K. L. Campman, and A. C. Gossard, Phys. Rev. Lett. **86**, 5608 (2001).

[48] L. V. Butov, A. C. Gossard, and D. S. Chemla, Nature (London) **418**, 751 (2002).

[49] L. V. Butov, J. Phys.: Condens. Matter **16**, R1577 (2004).

[50] D. Snoke, S. Denev, Y. Liu, L. Pfeiffer, and K. West, Nature (London) **418**, 754 (2002).

[51] S. Yang, A. T. Hammack, M. M. Fogler, L. V. Butov, and A. C. Gossard, Phys. Rev. Lett. **97**, 187402 (2006).

[52] L. V. Butov, J. Phys.: Condens. Matter **19**, 295202 (2007).

[53] M. Stern, V. Garmider, E. Segre, M. Rappaport, V. Umansky, Y. Levinson, and I. Bar-Joseph, Phys. Rev. Lett. **101**, 257402 (2008).

[54] A. J. Leggett, Rev. Mod. Phys. **73**, 307 (2001).

[55] H. Deng, G. Weihs, C. Santori, J. Bloch, and Y. Yamamoto, Science **298**, 199 (2002).

[56] C. W. Lai, N. Y. Kim, S. Utsunomiya, G. Roumpos, H. Deng, M. D. Fraser, T. Byrnes, P. Recher, N. Kumada, T. Fujisawa, and Y. Yamamoto, Nature (London) **450**, 529 (2007).

[57] R. Balili, V. Hartwell, D. Snoke, L. Pfeiffer, and K. West, Science **316**, 1007 (2007).

[58] H. Deng, G. S. Solomon, R. Hey, K. H. Ploog, and Y. Yamamoto, Phys. Rev. Lett. **99**, 126403 (2007).

[59] K. G. Lagoudakis, M. Wouters, M. Richard, A. Baas, I. Carusotto, R. André, L. S. Dang, and B. Deveaud-Plédran, Nat. Phys. **4**, 706 (2008).

[60] S. Utsunomiya, L. Tian, G. Roumpos, C. W. Lai, N. Kumada, T. Fujisawa, M. Kuwata-Gonokami, A. Löffler, S. Höfling, A. Forchel, and Y. Yamamoto, Nat. Phys. **4**, 700 (2008).

[61] A. Amo, D. Sanvitto, F. P. Laussy, D. Ballarini, E. del Valle, M. D. Martin, A. Lemaître, J. Bloch, D. N. Krizhanovskii, M. S. Skolnick, C. Tejedor, and L. Viña, Nature (London) **457**, 291 (2009).

[62] J. Keeling and N. G. Berloff, Nature (London) **457**, 273 (2009).

[63] M. Altarelli, Phys. Rev. B **28**, 842 (1983).

[64] K. Nilsson, A. Zakharova, I. Lapushkin, S. T. Yen, and K. A. Chao, Phys. Rev. B **74**, 075308 (2006).

[65] P. A. Folkes, G. Gumbs, W. Xu, and M. Taysing-Lara, Appl. Phys. Lett. **89**, 202113 (2006).

[66] J. Kono, B. D. McCombe, J.-P. Cheng, I. Lo, W. C. Mitchel, and C. E. Stutz, Phys. Rev. B **50**, 12242(R) (1994).

[67] J.-P. Cheng, J. Kono, B. D. McCombe, I. Lo, W. C. Mitchel, and C. E. Stutz, Phys. Rev. Lett. **74**, 450 (1995).

[68] J. Kono, B. D. McCombe, J.-P. Cheng, I. Lo, W. C. Mitchel, and C. E. Stutz, Phys. Rev. B **55**, 1617 (1997).

[69] H. Kitabayashi, T. Waho, and M. Yamamoto, Appl. Phys. Lett. **71**, 512 (1997).

[70] H. Ohno, L. Esaki, and E. E. Mendez, Appl. Phys. Lett. **60**, 3153 (1992).

[71] E. Halvorsen, Y. Galperin, and K. A. Chao, Phys. Rev. B **61**, 16743 (2000).

[72] I. B. Spielman, J. P. Eisenstein, L. N. Pfeiffer, and K. W. West, Phys. Rev. Lett. **84**, 5808 (2000).

[73] M. Kellogg, J. P. Eisenstein, L. N. Pfeiffer, and K. W. West, Phys. Rev. Lett. **93**, 036801 (2004).

[74] E. Tutuc, M. Shayegan, and D. A. Huse, Phys. Rev. Lett. **93**, 036802 (2004).

[75] D. B. Talley, L. B. Shaw, J. S. Sanghera, I. D. Aggarwal, A.

Cricenti, R. Generosi, M. Luce, G. Margaritondo, J. M. Gilligan, and N. H. Tolk, Mater. Lett. **42**, 339 (2000).

[76] J.-S. Samson, G. Wollny, E. Bründermann, A. Bergner, A. Hecker, G. Schwaab, A. D. Wieck, and M. Havenith, Phys. Chem. Chem. Phys. **8**, 753 (2006).

[77] L. M. Claessen, J. C. Maan, M. Altarelli, P. Wyder, L. L. Chang, and L. Esaki, Phys. Rev. Lett. **57**, 2556 (1986).

[78] G. M. Sundaram, R. J. Warburton, R. J. Nicholas, G. M. Summers, N. J. Mason, and P. J. Walker, Semicond. Sci. Technol. **7**, 985 (1992).

[79] J.-C. Chiang, S.-F. Tsay, Z. M. Chau, and I. Lo, Phys. Rev. Lett. **77**, 2053 (1996).

[80] M. J. Yang, C. H. Yang, B. R. Bennett, and B. V. Shanabrook, Phys. Rev. Lett. **78**, 4613 (1997).

[81] M. Lakrimi, S. Khym, R. J. Nicholas, D. M. Symons, F. M. Peeters, N. J. Mason, and P. J. Walker, Phys. Rev. Lett. **79**, 3034 (1997).

[82] T. P. Marlow, L. J. Cooper, D. D. Arnone, N. K. Patel, D. M. Whittaker, E. H. Linfield, D. A. Ritchie, and M. Pepper, Phys. Rev. Lett. **82**, 2362 (1999).

[83] Y. Vasilyev, S. Suchalkin, K. von Klitzing, B. Meltser, S. Ivanov, and P. Kop'ev, Phys. Rev. B **60**, 10636 (1999).

[84] A. J. L. Poulter, M. Lakrimi, R. J. Nicholas, N. J. Mason, and P. J. Walker, Phys. Rev. B **60**, 1884 (1999).

[85] C. Petchsingh, R. J. Nicholas, K. Takashina, N. J. Mason, and J. Zeman, Physica E **12**, 289 (2002).

[86] K. Suzuki, S. Miyashita, and Y. Hirayama, Phys. Rev. B **67**, 195319 (2003).

[87] C. Petchsingh, R. J. Nicholas, K. Takashina, N. J. Mason, and J. Zeman, Phys. Rev. B **70**, 155306 (2004).

[88] C. Petchsingh, R. J. Nicholas, K. Takashina, and N. J. Mason, Semicond. Sci. Technol. **22**, 194 (2007).

[89] D. Heitman, M. Ziesmann, and L. L. Chang, Phys. Rev. B **34**, 7463R (1986).

[90] H. Bluyssen, J. C. Maan, P. Wyder, L. l. Chang, L. Esaki, Solid State Commun. **31**, 35 (1979).

[91] Y. Guldner, J. P. Vieren, P. Voisin, M. Voos, L. L. Chang, and L. Esaki, Phys. Rev. Lett. **45**, 1719 (1980).

[92] J. C. Maan, Y. Guldner, J. P. Vieren, P. Voisin, M. Voos, L. L. Chang, and L. Esaki, Solid State Commun. **39**, 683 (1981).

[93] J. C. Maan, C. Uihlein, L. L. Chang, and L. Esaki, Solid State Commun. **44**, 653 (1982).

[94] H. J. A. Bluyssen, J. C. Maan, P. Wyder, L. L. Chang, and L. Esaki, Phys. Rev. B **25**, 5364 (1982).

[95] E. E. Mendez, L. Esaki, and L. L. Chang, Phys. Rev. Lett. **55**, 2216 (1985).

[96] M. S. Daly, K. S. H. Dalton, M. Lakrimi, N. J. Mason, R. J. Nicholas, M. van der Burgt, P. J. Walker, D. K. Maude, and J. C. Portal, Phys. Rev. B **53**, R10524 (1996).

[97] R. J. Nicholas, K. Takashina, M. Lakrimi, B. Kardynal, S. Khym, N. J. Mason, D. M. Symons, D. K. Maude, and J. C. Portal, Phys. Rev. Lett. **85**, 2364 (2000).

[98] K. Takashina, R. J. Nicholas, B. Kardynal, N. J. Mason, D. K. Maude, and J. C. Portal, Phys. Rev. B **68**, 235303 (2003).

[99] J. M. Ziman, *Principles of the Theory of Solids*, 2nd ed. (Cambridge University Press, London, 1972), p. 250.

[100] This energy is close to the values obtained in several theoretical calculations, Refs. 26, 27, and 64.

[101] J. Kono and B. D. McCombe, Phys. Rev. Lett. **80**, 2497 (1998).

[102] T. Ando, A. B. Fowler, and F. Stern, Rev. Mod. Phys. **54**, 437 (1982).

[103] J. M. Heisz and E. Zaremba, Semicond. Sci. Technol. **8**, 575 (1993).

[104] Z. Schlesinger, J. C. M. Hwang, and S. J. Allen, Phys. Rev. Lett. **50**, 2098 (1983).

[105] M. J. Yang, R. J. Wagner, B. V. Shanabrook, J. R. Waterman, and W. J. Moore, Phys. Rev. B **47**, 6807 (1993).

[106] J. Scriba, A. Wixforth, J. P. Kotthaus, C. R. Bolognesi, C. Nguyen, G. Tuttle, J. H. English, and H. Kroemer, Semicond. Sci. Technol. **8**, S133 (1993).

[107] T. Englert, J. C. Maan, C. Uihlein, D. C. Tsui, and A. C. Gossard, Solid State Commun. **46**, 545 (1983).

[108] T. Ando, J. Phys. Soc. Jpn. **38**, 989 (1975).

[109] S. Das Sarma, Phys. Rev. B **23**, 4592 (1981).

[110] R. Lassnig and E. Gornik, Solid State Commun. **47**, 959 (1983).

[111] E. B. Hansen and O. P. Hansen, Solid State Commun. **66**, 1181 (1988).

[112] V. Piazza, V. Pellegrini, F. Beltram, W. Wegscheider, T. Jungwirth, and A. H. MacDonald, Nature (London) **402**, 638 (1999).

[113] W. Kohn and D. Sherrington, Rev. Mod. Phys. **42**, 1 (1970).

[114] H.-J. Mikeska and H. Schmidt, Z. Phys. B **20**, 43 (1975).

[115] J. P. Kotthaus, G. Abstreiter, J. f. Koch, and R. Ranvaud, Phys. Rev. Lett. **34**, 151 (1975).

[116] J.-P. Cheng and B. D. McCombe, Phys. Rev. Lett. **64**, 3171 (1990).

[117] J. Richter, H. Sigg, K. v. Klitzing, and K. Ploog, Phys. Rev. B **39**, 6268 (1989).

[118] C. K. Kallin and B. I. Halperin, Phys. Rev. B **31**, 3635 (1985).